NASA TECHNICAL MEMORANDUM

NASA TM X-3542

CORRELATION OF PART-SPAN DAMPER LOSSES THROUGH TRANSONIC ROTORS OPERATING NEAR DESIGN POINT

William B. Roberts

Lewis Research Center
Cleveland, Ohio 44135

NATIONAL AERONAUTICS AND SPACE ADMINISTRATION • WASHINGTON, D. C. • JUNE 1977

1. Report No.	2. Government Accession No.	3. Recipient's Catalog No.
NASA TM X-3542		

4. Title and Subtitle	5. Report Date
CORRELATION OF PART-SPAN DAMPER LOSSES THROUGH TRANSONIC ROTORS OPERATING NEAR DESIGN POINT	June 1977
	6. Performing Organization Code
7. Author(s)	8. Performing Organization Report No.
William B. Roberts	E-9068
	10. Work Unit No.
9. Performing Organization Name and Address	505-04
Lewis Research Center National Aeronautics and Space Administration Cleveland, Ohio 44135	11. Contract or Grant No.
	13. Type of Report and Period Covered
12. Sponsoring Agency Name and Address	Technical Memorandum
National Aeronautics and Space Administration Washington, D. C. 20546	14. Sponsoring Agency Code

15. Supplementary Notes

16. Abstract

The design-point losses caused by part-span dampers (PSD) were correlated for 21 transonic axial-flow fan rotors that had tip speeds varying from 350 to 488 meters per second and design pressure ratios of 1.5 to 2.0. For these rotors a correlation using mean inlet Mach number at the damper location, along with relevant geometric and aerodynamic loading parameters, predicts the variation of total pressure loss coefficient in the region of the damper to a good approximation.

17. Key Words (Suggested by Author(s))	18. Distribution Statement
Dampers Losses Transonic compressors Shrouds	Unclassified - unlimited STAR category 02

19. Security Classif. (of this report)	20. Security Classif. (of this page)	21. No. of Pages	22. Price*
Unclassified	Unclassified	22	A02

* For sale by the National Technical Information Service, Springfield, Virginia 22161

CORRELATION OF PART-SPAN DAMPER LOSSES THROUGH TRANSONIC ROTORS OPERATING NEAR DESIGN POINT

by William B. Roberts*

Lewis Research Center

SUMMARY

The design-point losses caused by part-span dampers (PSD) were correlated for 21 transonic axial-flow fan rotors that had tip speeds varying from 350 to 488 meters per second and design pressure ratios of 1.5 to 2.0. The additional loss attributable to the damper and the total region along the blade height influenced were correlated with selected aerodynamic and geometric parameters. The maximum damper loss correlated well with the mean inlet Mach number at the damper location, the geometric parameters of leading- and trailing-edge damper radius normalized by mean passage height and damper aerodynamic chord, respectively, and the aerodynamic loading parameter of the blade camber divided by the solidity at the damper location. The region of damper influence extended over a mean passage height of the order of 10 to 15 times the maximum damper thickness.

INTRODUCTION

Modern fan-jet aircraft engines require high-pressure-ratio, high-bypass fan stages of short axial length to minimize weight and internal and external nacelle drag. This leads to high-aspect-ratio, high-speed transonic blading that often necessitates the use of one or more part-span dampers (PSD) for structural integrity. Figure 1 shows the part-span damper geometry and typical damper profiles. The need for high thermal efficiency through these engines makes it desirable to have a method to predict the localized losses caused by the dampers. This localized loss region is illustrated in figure 2.

The usual method of accounting for the damper loss has been to increase the average

*Assistant Professor of Aerospace and Mechanical Engineering, University of Notre Dame, Notre Dame, Indiana; Summer Faculty Fellow at the Lewis Research Center in 1976.

overall blade loss a certain amount to account for the expected decrease in performance. However, this technique does not consider the large temperature and pressure gradients in the region of the damper. Furthermore, the blockage and losses associated with the damper cause significant flow shifts toward the end-wall regions that can adversely affect performance over the entire blade passage. Finally, the stator blading is often strongly affected, particularly in the region directly behind the damper, due to the maldistribution of flow from the rotor. Consequently, it would be beneficial to be able to predict the losses due to the dampers and their regions of influence; then the effects on localized and overall performance can be calculated and minimized if possible.

In reference 1, Esgar and Sandercock have shown that performance over the blade height can be predicted if the total pressure loss distribution is known in the region of the damper. They took the measured values of energy addition and loss from several transonic rotors with dampers and used these data to calculate the variation of outlet velocity, flow angle, and pressure over the blade span. A typical result is given in figure 3. However, the pressure loss distribution in the damper region is not generally known before experimental data are obtained. The data from several rotors with part-span dampers are examined and correlated herein with selected aerodynamic and geometrical parameters to give a method of predicting the localized damper influence at the design point.

FACTORS AFFECTING DAMPER LOSSES

The losses through transonic rotors caused by part-span dampers can be attributed to several aerodynamic and geometric factors: Mach number, damper angle of attack, maximum damper thickness and aerodynamic chord, leading- and trailing-edge thickness, blade span in relation to the damper geometry, and the blade geometry at the damper location. In reference 2, Benser, et al., described experiments done on shock wave visualization by laser hologram in the damper region of a high-tip-speed transonic fan rotor. Figure 4 is a view of a transmitted light hologram image coincident with the rotor blade, and figure 5 shows the interpreted shock system for this rotor at design speed and near-design pressure ratio. There is the expected blade leading-edge passage shock, but there are also two shock waves that have been caused by the damper. The first shock starts from the damper leading edge at the blade suction surface and wraps around the damper at an angle to the remainder of the leading edge, and the second comes from the junction of adjacent dampers. Both shocks propagate radially toward the tip. (It is assumed that a similar radial propagation of the shocks occurs toward the hub.) Figures 2 and 3 show that the loss caused by the damper does not occur in a sharp spike, but with a maximum loss at the shroud location and a gradual decrease of loss on either side. The radial propagation of shock waves from the damper, decreasing in in-

tensity with distance, is the probable cause of this, as the damper wake could be expected to be relatively small[1] and there would be little mixing measured by a probe placed immediately downstream of the rotor. The strength of the leading-edge damper shock is a function of the Mach number at the damper leading edge, the leading-edge thickness, and the deflection angle (if the damper operates at a nonzero angle of attack). The second shroud shock appears to be caused by the ill fit of the damper bearing surfaces. Therefore, the strength of this shock depends on the damper surface Mach number and the radial position of the dampers with respect to each other.

The magnitude of the profile or wake loss is a function of the angle of attack of the damper with respect to the stream surface intersecting the leading edge, the relative thickness of the trailing edge, and pressure gradients caused by the local blade-to-blade circulation (loading). At zero or near-zero angle of attack the profile loss can be expected to be lower than the shock losses for relatively thin dampers. However, the wake loss will increase proportionately with the thickness of the trailing edge.

It is clear that the flow in the region of the damper is highly complex and three dimensional in nature. An analytical solution of this flow field would require the ability to calculate in three dimensions and would include the effects of viscosity. Presently, this is not practical. Therefore, an experimental correlation considering the relevant physical parameters must be used to predict losses in the region of the part-span damper.

LOSS CORRELATIONS

To develop a meaningful experimental correlation for part-span damper losses, it is necessary to have a large body of data to draw upon. Fortunately, the Lewis Research Center of the National Aeronautics and Space Administration has tested over 40 research rotors during the past decade, more than half of which were transonic fans with part-span dampers. The data from 19 of these tests were available for use in the present correlation, all but one using the NASA type B damper that consists of a symmetrical double-circular-arc profile set along the design stream surface. Only one rotor used the type A damper, for it was found to cause very high losses. These two damper profiles are shown in figure 1.

The damper loss region was well defined in the NASA tests by five data points taken in the immediate vicinity of the damper, approximately one-half of a chord length downstream. Figure 6 shows a typical radial variation of total pressure loss coefficient for NASA rotor 16 and demonstrates how the maximum damper loss coefficient $\overline{\omega}_{PSD,M}$

[1]The damper was located along a design stream surface and the rotor was operating very near design point. Therefore, angle of attack would be expected to be near zero.

and region of influence were estimated by fairing the radial distribution of the loss coefficient across the damper region as if it were not present. It can be seen that the lack of a data point at 80 percent of span could introduce some error into the estimate of damper maximum loss. If at 80 percent of span the loss coefficient was near the design value (~0.07), the estimate of maximum damper loss coefficient would be in error by ~0.01. This is typical of most of the data, that is, the estimates of maximum loss coefficient due to the damper were accurate to ±0.01. These loss estimates were made for all 19 of the NASA rotors at 100 percent of design speed and maximum measured efficiency. A perusal of the data showed that losses in the damper region were minimum at this test condition and that the damper would be operating at or near zero angle of attack. This was important for the data were reduced in such a way that an angle-of-attack value was not available. All pertinent data and references for these rotors, along with correlation parameters that will be discussed, are listed in table I. The damper geometry for each rotor was taken from design drawings or measured if necessary.

Data were sought from NASA-sponsored industrial research for fan rotors with dampers to include in the correlation. A search revealed two rotors with sufficient loss definition in the damper region to be included herein. One was the first-stage rotor from a Pratt & Whitney two-stage transonic fan, the other was the single-stage rotor used in the holographic studies mentioned earlier, which was designed and tested by AiResearch. The shapes of the dampers from these two rotors, types C and D, respectively, are shown in figure 1; other pertinent data are given in table I.

For all of the data, the location of the maximum loss in the damper region occurred within 2 percent of span (at the trailing edge) of the damper location, indicating that there were no significant radial shifts in the near wake downstream of these rotors.

After the data were assembled, the maximum loss coefficient of the experimental damper and the aerodynamic and geometric data were correlated. Several preliminary correlations indicated that shock and profile losses should be additive in the following form:

$$\overline{\omega}_{PSD,\,M} = f_1\left(\overline{M},\ \frac{r_{le}}{t}\right) + f_2\left(\frac{t}{c_d}\right) \tag{1}$$

(Symbols are defined in the appendix.) The damper inlet Mach number varies across the blade spacing because of the flow expansion over the uncovered portion of the blade suction surface, or flow compression in the case of a "precompression" shaped rotor blade. It is assumed that the damper mean inlet Mach number is the same as that used to calculate the passage shock loss, which is computed from the methods of reference 3. Reid and Urasek (ref. 4) have shown that shock detachment distance and strength for rotor blades depends on the relative thickness or bluntness of the leading edge for any

given Mach number, hence the term r_{le}/t. The strength of the second damper shock depends on the mismatch of the bearing surfaces for various running speeds and as such would be very difficult to assess. Since the damper surface Mach number should be less than the inlet Mach number for most transonic flows, it was thought that the loss due to this shock would be secondary to that caused by the inlet shock system. Therefore, because of the difficulty involved in evaluating this type of loss, it was assumed to be much less than the inlet shock loss. The damper profile loss was correlated on the basis of the relative thickness t/c_d.

Expressions based on equation (1) did show correlation; however, there was considerable data scatter. Three factors that had not been taken into account in the first attempts at correlation were the flow blockage caused by the damper, the effect of the damper trailing-edge relative thickness on profile loss, and the effect of local pressure gradients due to blade loading on damper boundary layer and wake. Several modified expressions were correlated which took these factors into account:

$$\overline{\omega}_{PSD,\,M} = f_1'\left(\overline{M},\ \frac{r_{le}}{t},\ \frac{t}{h}\right) + f_2'\left(\frac{t}{c_d},\ \frac{r_{le}}{t},\ \varphi,\ \sigma\right) \tag{2}$$

The final form, giving the best correlation, was

$$\overline{\omega}_{PSD,\,M} = K_1\left(\frac{r_{le}}{t}\right)\left(\frac{t}{h}\right)\overline{\omega}_s + K_2\left(\frac{t}{c_d}\right)\left(\frac{r_{te}}{t}\right)\frac{\varphi}{\sigma}$$

which reduces to

$$\overline{\omega}_{PSD,\,M} = K_1\left(\frac{r_{le}}{h}\right)\overline{\omega}_s + K_2\left(\frac{r_{te}}{c_d}\right)\frac{\varphi}{\sigma} \tag{3}$$

where $\overline{\omega}_s$ is the normal shock loss at $\overline{M}$. Calibration of equation (3) with the data given in table I resulted in the following values for the constants:

$$\left.\begin{aligned} K_1 &= 500 \\ \text{and} \\ K_2 &= 8 \end{aligned}\right\} \tag{4}$$

Figure 7 compares the $\overline{\omega}_{PSD,\,M}$ calculated by equation (3) with that estimated from the

experimental data. All but four data points fall within the expected accuracy band. This tends to substantiate the assumption that any second shock formed from the relative displacement of the dampers was weaker than the primary shock. Scatter outside the expected accuracy band could be caused by significant mismatch of the damper bearing surfaces or by variance of damper geometry outside of tolerance.

The fraction of the span influenced by the damper was estimated from the experimental data. This was correlated with the damper blockage factor t/h, which is given in table I. The correlation is shown in figure 8. The tolerance on the experimental values is due to the lack of data points near the ends of the damper region of influence. This correlation indicates that the damper affects the rotor loss over a spanwise distance of approximately 10 to 15 times the damper maximum thickness. For further use in the general correlation, the fraction of spanwise influence was taken as 12.5 times the normalized damper maximum thickness,

$$\frac{x}{h} = 12.5\,\frac{t}{h} \tag{5}$$

which fits near the mean for most of the data.

An inspection of the data showed that the variation of damper loss coefficient in the region of influence could be approximated by a modified normal distribution of the following type:

$$\left.\begin{aligned} \overline{\omega}_{DR} &= f(x, \overline{\omega}_{DR,\,M}) \\ \overline{\omega}_{DR} &= (\overline{\omega}_{DR,\,M} - \overline{\omega}_{o})\left[e^{-2(2d/x)^{2}} - e^{-2(x/2d)^{100}}\right] + \overline{\omega}_{o} \end{aligned}\right\} \tag{6}$$

where $\overline{\omega}_{DR,\,M} = \overline{\omega}_{o,\,M} + \overline{\omega}_{PSD,\,M}$. This spanwise variation is illustrated in figure 9, where it is seen that equation (6) must be applied to both the hub and tip sides of the damper.

Equations (3) to (6) were used to calculate the variation of loss in the part-span damper region for 10 rotors selected from table I. Rotors were used that had a wide variation of damper size and aerodynamic loading. The spanwise location of the maximum loss was assumed to be directly downstream of the damper as viewed from the trailing edge. These calculations were then compared with experiment, as shown in figure 10. The agreement between correlation and experiment was generally good. For the worst case the maximum loss coefficient in the damper region was predicted low by 0.03, representing ~16 percent of the experimental value (fig. 10(b)). It is more difficult to determine the agreement between calculated and experimental values in the

damper region of influence due to the lack of data. However, for the rotors used in figure 10 the agreement was fair to good.

LOSSES AT OFF-DESIGN CONDITIONS

The correlation represented by equations (3) to (6) was calibrated with data taken from rotors operating at or near maximum efficiency at design speed. The lowest damper losses often occur at or near the design point because the dampers are usually set along design stream surfaces and, consequently, should operate at or near zero angle of attack. At off-design conditions, there is a change in the damper angle of attack that could increase the flow deflection at the leading edge, which would increase the strength of the inlet shock. Although the available data do not allow an estimate of damper angle of attack, a qualitative idea of off-design performance can be had by plotting damper maximum loss $\overline{\omega}_{PSD,\,M}$ and region of influence x/h with corrected weight flow. This was done for NASA rotors 4 and 16 and is shown in figure 11. It can be seen that the loss and the region of influence can vary significantly with weight flow. A minimum occurs at or near the maximum efficiency point and, at this weight flow and below, the prediction of $\overline{\omega}_{PSD,\,M}$ is fair. However, at higher weight flows the predicted loss is much too low. Finally, for both rotors the present correlation greatly underestimates the region of influence at off-design points. For these reasons, this correlation is most useful in the vicinity of the design point.

DISCUSSION

As figure 3 indicates, a good estimate of the loss variation in the damper region of influence makes possible an accurate calculation of blade row performance over the span. The loss in the damper region must be taken into account on an iterative basis since the aerodynamic forces and the blade geometry must be known before the required damper size can be calculated. After this, the effect of the damper on performance is most easily determined by using the present correlation in a "direct" calculation method, where a given geometry is analyzed to determine aerodynamic performance. It is possible to use the correlation iteratively in an "indirect" or design method, but care must be exercised in the original specification of spanwise rotor outlet pressure and temperature to insure that the output is physically realistic. Iteration procedures for design (indirect) or analysis (direct) methods can be calibrated by using experimental data from rotors with dampers, as long as the data through the damper region are well defined.

Knowledge of the spanwise flow variation behind the damper makes it possible to

minimize the impact of the damper and its associated losses on performance. It also allows trade-off studies to be made between high-aspect-ratio rotors with dampers and rotors of lower aspect ratio without dampers.

CONCLUDING REMARKS

A correlation has been made between part-span damper losses and blade element design-point aerodynamic and geometric data using 21 transonic axial-flow research rotors that varied greatly in tip speed and loading. The maximum total pressure losses attributable to the damper were correlated with the following parameters:

(1) The shock loss coefficient $\overline{\omega}_s$ for the blade passage containing the damper, which is the total pressure loss coefficient associated with a normal shock of strength $\overline{M}$

(2) A blade aerodynamic loading parameter, the camber divided by the solidity φ/σ at the damper spanwise location

(3) The leading- and trailing-edge damper radius normalized by the mean span and damper chord, respectively, r_{le}/h and r_{te}/c_d.

The tightest data correlation was obtained from the combination of parameters given by

$$\overline{\omega}_{PSD,\,M} = 500\left(\frac{r_{le}}{h}\right)\overline{\omega}_s + 8\left(\frac{r_{te}}{c_d}\right)\frac{\varphi}{\sigma}$$

Examination of the data from the research rotors revealed that the spanwise region influenced extended over 10 to 15 times the damper maximum thickness, symmetrically around the damper to a good approximation. For the present correlation a value of 12.5 times the normalized damper thickness was chosen to estimate the spanwise region of influence.

The variation of loss in the damper region of influence can be approximated by a modified normal distribution given by the equation

$$\overline{\omega}_{DR} = (\overline{\omega}_{DR,\,M} - \overline{\omega}_o)\left[e^{-2(2d/x)^2} - e^{-2(x/2d)^{100}}\right] + \overline{\omega}_o$$

This correlation should be quite useful in the design of transonic axial-flow fan and compressor rotors that must use part-span dampers for structural integrity. It allows an estimate to be made of the local loss variation in the vicinity of the damper. Using

this variation allows the local and overall effects of the damper on the spanwise distribution of pressure, temperature, velocity, efficiency, and flow angle to be computed.

Lewis Research Center,
National Aeronautics and Space Administration,
Cleveland, Ohio, February 23, 1977,
505-04.

APPENDIX - SYMBOLS

c	blade chord, cm
c_d	part-span damper chord, cm
D	diffusion factor
d	distance between spanwise location of $\overline{\omega}_{PSD, M}$ and end of damper region of influence, either toward hub or tip, cm
h	mean blade span height, cm
K_1, K_2	constants
$\overline{M}$	mean inlet Mach number, average of inlet Mach number ahead of blade and maximum suction-surface Mach number calculated by method of ref. 3
r	spanwise radius in meridional plane
r_{le}	leading-edge part-span damper radius, cm
r_{te}	trailing-edge part-span damper radius, cm
t	part-span damper thickness, cm
x	part-span damper spanwise region of influence, cm
σ	solidity, ratio of blade chord to spacing
φ	camber angle, radians
$\overline{\omega}$	total pressure loss coefficient

Subscripts:

DR	damper region
DR, M	maximum loss in damper region
d	damper
h	hub
M	location of maximum damper loss
max	maximum
o	estimated loss level in absence of a part-span damper
PSD, M	maximum additional loss due to part-span damper (fig. 6)
s	normal shock
t	tip

REFERENCES

1. Esgar, Genevieve M.; and Sandercock, Donald M.: Some Observed Effects of Part-Span Dampers on Rotating Blade Row Performance Near Design Point. NASA TM X-2696, 1973.

2. Benser, W. A.; Bailey, E. E.; and Gelder, T. F.: Holographic Studies of Shock Waves within Transonic Fan Rotors. J. Eng. Power, vol. 97, series A, no. 1, Jan. 1975, pp. 75-84.

3. Schwenk, Francis C.; Lewis, George W.; and Hartmann, Melvin J.: A Preliminary Analysis of the Magnitude of Shock Losses in Transonic Compressors. NACA RM E57A30, 1957.

4. Reid, Lonnie; and Urasek, Donald C.: Effects of Increased Leading Edge Thickness on Performance of a Transonic Rotor Blade In Single-Stage Transonic Compressor. NASA TN D-7489, 1973 (also see ASME Paper 73-GT-60).

5. Reid, Lonnie; and Tysl, Edward R.: Performance of a Transonic Compressor Rotor with an Aspect Ratio of 6.5. NASA TN D-7662, 1974.

6. Hager, Roy D.; Janetzke, David C.; and Reid, Lonnie: Performance of a 1380-Foot-Per-Second-Tip-Speed Axial-Flow Compressor Rotor with a Blade Tip Solidity of 1.3. NASA TM X-2448, 1972.

7. Lewis, George W., Jr.; and Urasek, Donald C.: Comparison of the Effect of Two Damper Sizes on the Performance of a Low-Solidity Axial-Flow Transonic Compressor Rotor. NASA TM X-2536, 1972.

8. Janetzke, David C.; Ball, Calvin L.; and Hager, Roy D.: Performance of 1380-Foot-Per-Second Tip-Speed Axial-Flow Compressor Rotor with Blade Tip Solidity of 1.1. NASA TM X-2449, 1972.

9. Ball, Calvin L.; Janetzke, David C.; and Reid, Lonnie: Performance of 1380-Foot-Per-Second-Tip-Speed Axial-Flow Compressor Rotor with Blade Tip Solidity of 1.5. NASA TM X-2379, 1972.

10. Kovich, George; and Reid, Lonnie: Overall and Blade-Element Performance of a Multiple-Circular-Arc Bladed Transonic Compressor Rotor with Tip Speed of 1375 Feet Per Second. NASA TM X-2697, 1973.

11. Urasek, Donald C.; and Janetzke, David C.: Performance of Tandem-Bladed Transonic Compressor Rotor with Tip Speed of 1375 Feet Per Second. NASA TM X-2484, 1972.

12. Osborn, Walter M.; Urasek, Donald C.; and Moore, Royce D.: Performance of a Single-Stage Transonic Compressor with a Blade-Tip Solidity of 1.5 and Comparison with 1.3- and 1.7-Solidity Stages. NASA TM X-2926, 1973.

13. Kovich, George; Moore, Royce D.; and Urasek, Donald C.: Performance of Transonic Fan Stage with Weight Flow per Unit Annulus Area of 198 Kilograms Per Second Per Square Meter (40.6 (lb/sec)/ft^2). NASA TM X-2905, 1973.

14. Moore, Royce D.; and Reid, Lonnie: Performance of a Single-Stage Axial-Flow Transonic Compressor Stage with a Blade Tip Solidity of 1.7. NASA TM X-2658, 1972.

15. Urasek, Donald C.; Moore, Royce D.; and Osborn, Walter M.: Performance of a Single-Stage Transonic Compressor with a Blade-Tip Solidity of 1.3. NASA TM X-2645, 1972.

16. Moore, Royce D.; Urasek, Donald C.; and Kovich, George: Performance of Transonic Fan Stage with Weight Flow per Unit Annulus Area of 178 Kilograms Per Second Per Square Meter (36.5 (lb/sec)/ft^2). NASA TM X-2904, 1973.

17. Lewis, George W., Jr.; Reid, Lonnie; and Tysl, Edward R.: Design and Performance of a High-Pressure-Ratio, Highly Loaded Axial-Flow Transonic Compressor Stage. NASA TM X-3100, 1974.

18. Urasek, Donald C.; Steinke, Ronald J.; and Lewis, George W., Jr.: Performance of Inlet Stage of Transonic Compressor. NASA TM X-3345, 1976.

19. Messenger, H. E.; and Keenan, M. J.: Two-Stage Fan. 2: Data and Performance with Redesigned Second-Stage-Rotor Uniform and Distorted Inlet Flows. (PWA-5087, Pratt & Whitney Aircraft; NAS3-13494) NASA CR-134710, 1974.

20. Ware, T. C.; Kobayaski, R. J.; and Jackson, R. J.: High-Tip-Speed, Low-Loading Transonic Fan Stage. Part 3: Final Report. (AiResearch-73-9488-Pt-3, AiResearch Mfg. Co.; NAS3-13498) NASA CR-121263, 1974.

TABLE I. - DATA FOR PART-SPAN DAMPER CORRELATIONS

Rotor	Damper profile type (from fig. 1)	Location of maximum part-span damper loss, r_{te}, percent of span at trailing edge	Leading- and trailing-edge part-span damper radius normalized with respect to -		Part-span damper maximum thickness normalized with respect to mean span height, t/h	Mean Mach number at part-span damper location, $\overline{M}$	Blade camber at part-span damper location, φ, rad	Blade solidity at part-span damper location, σ	Maximum total pressure loss coefficient due to part-span damper, $\overline{\omega}_{PSD, M}$		Reference	Experimental reading	Symbol used in figures
			Mean span height, r/h	Part-span damper chord, r/c_d					Calculated	Estimated from experiment			
NASA 2	A	32.5	0.0110	0.1200	0.0217	1.25	0.228	1.66	0.246	0.230	5	309	○
NASA 2, Mod-1	B	33.1	.0021	.0324	.0173	1.25	.245	1.66	.060	.087	5	1058	□
NASA 3		45.0	.0034	.0135	.0344	1.43	.225	1.64	.125	.128	6	532	◇
NASA 3, Mod-1		45.0	.0023	.0242	.0172	1.41	.214	1.66	.095	.109	7	20	△
NASA 4		45.0		.0265		1.45	.190	1.39	.118	.120	8	919	◺
NASA 5		43.0		.0255		1.39	.213	1.82	.090	.071	9	992	⬠
NASA 6		47.5		.0259		1.37	.192	1.66	.084	.083	10	198	⬠
NASA 7		45.0		.0255		1.38	.185	1.63	.076	.070	11	127	◇
NASA 8		50.0		.0259	.0170	1.36	.226	1.86	.074	.078	12	59	◇
NASA 11		55.0	.0022	.0223	.0184	1.33	.116	1.69	.056	.076	13	969	⬠
NASA 12		50.0	.0023	.0199	.0189	1.36	.222	2.16	.069	.075	14	305	▽
NASA 14		50.0	.0023	.0180	.0191	1.34	.257	1.65	.072	.084	15	341	◹
NASA 16		55.0	.0022	.0209	.0183	1.27	.140	1.71	.041	.046	16	1060	⬡
NASA 18		55.0	.0023	.0262	.0190	1.35	.426	2.21	.095	.100	17	927	⬡
NASA 19		60.0	.0022	.0204	.0187	1.34	.159	1.73	.063	.070	(a)	2723	○
NASA 20		60.0	.0022	.0192	.0180	1.29	.123	1.76	.046	.047	(a)	2918	◇
NASA 66		46.0	.0021	.0220	.0150	1.32	.097	1.77	.047	.050	18	867	⬡
NASA 2S-SD		42.0	.0018	.0218	.0149	1.26	.175	1.68	.037	.045	(a)	190	◁
NASA 2S-LD		50.0	.0053	.0405	.0354	1.23	.230	1.78	.098	.095	(a)	16	▷
P & WA	C	60.0	.0047	.0160	.0234	[b]~1.30	.280	1.51	.101	.101	19	3-10-03	◇
AiResearch	D	30.0	.0015	.0072	.0192	[c]~1.51	.072	1.69	.085	.100	20	128	⬡

[a]Unpublished NASA data.

[b]Shock losses taken from reference.

[c]$\overline{M}$ estimated from data in reference.

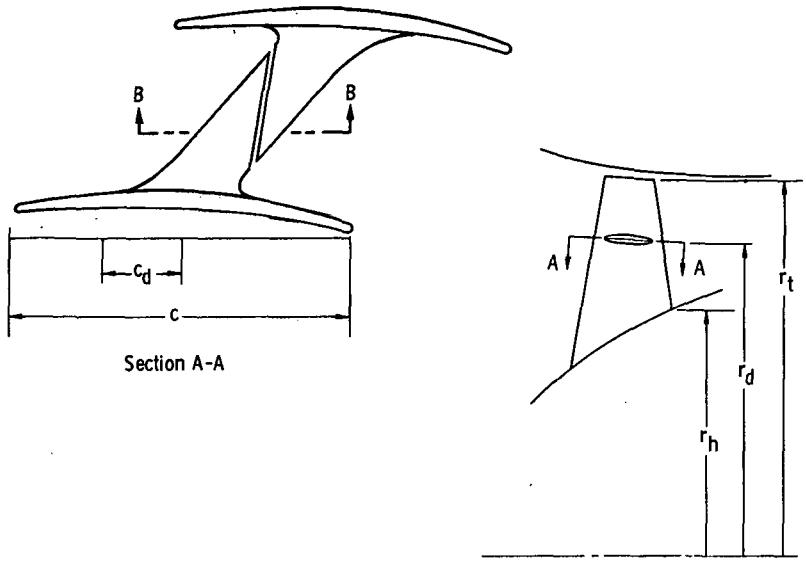

Section A-A

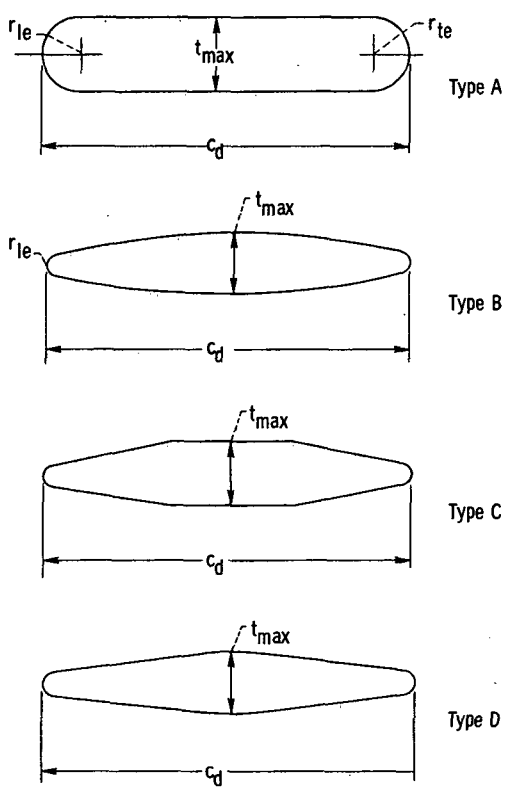

Section B-B: Damper profiles used in correlation

Figure 1. - Geometry of part-span dampers.

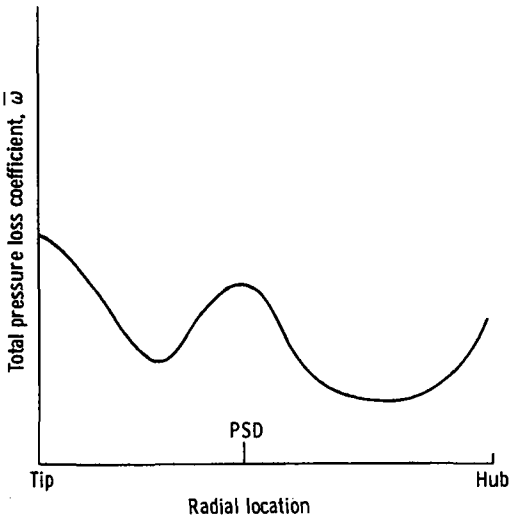

Figure 2. - Radial variation of total pressure loss coefficient for rotor with part-span damper (PSD).

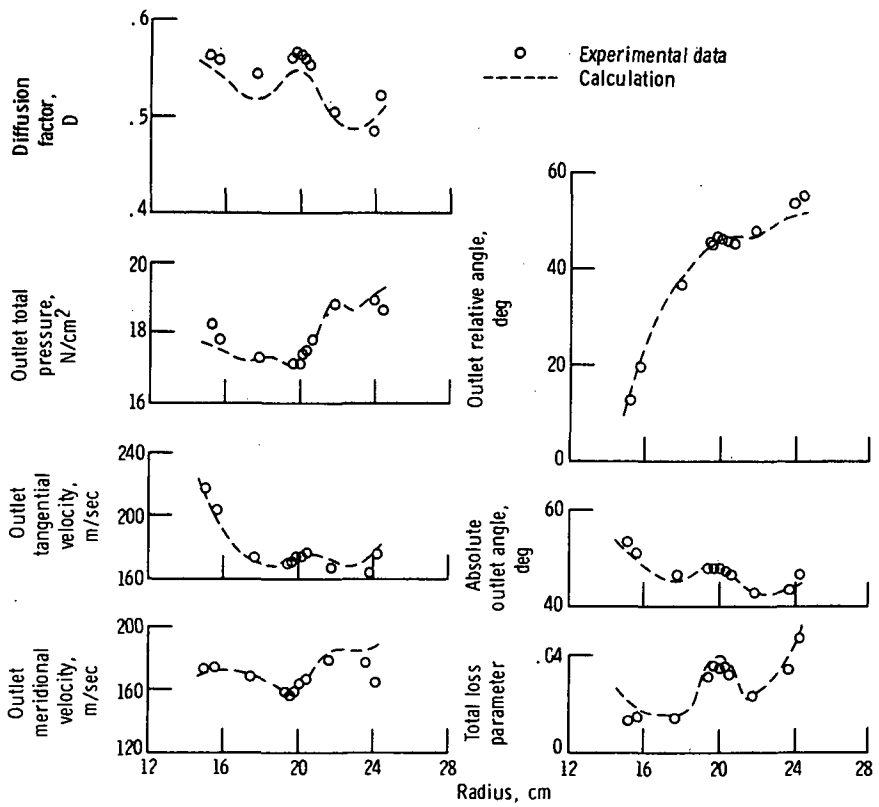

Figure 3. - Comparison of measured parameters with computed values using measured energy addition and losses including local damper loss.

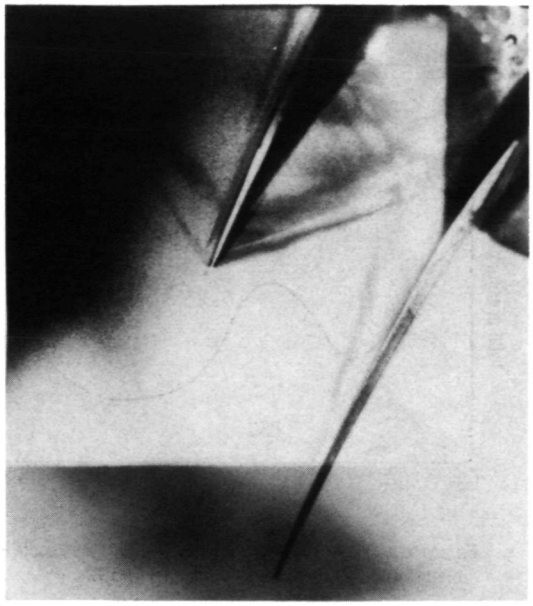

Figure 4. - View of transmitted light hologram image coincident with rotor blades.

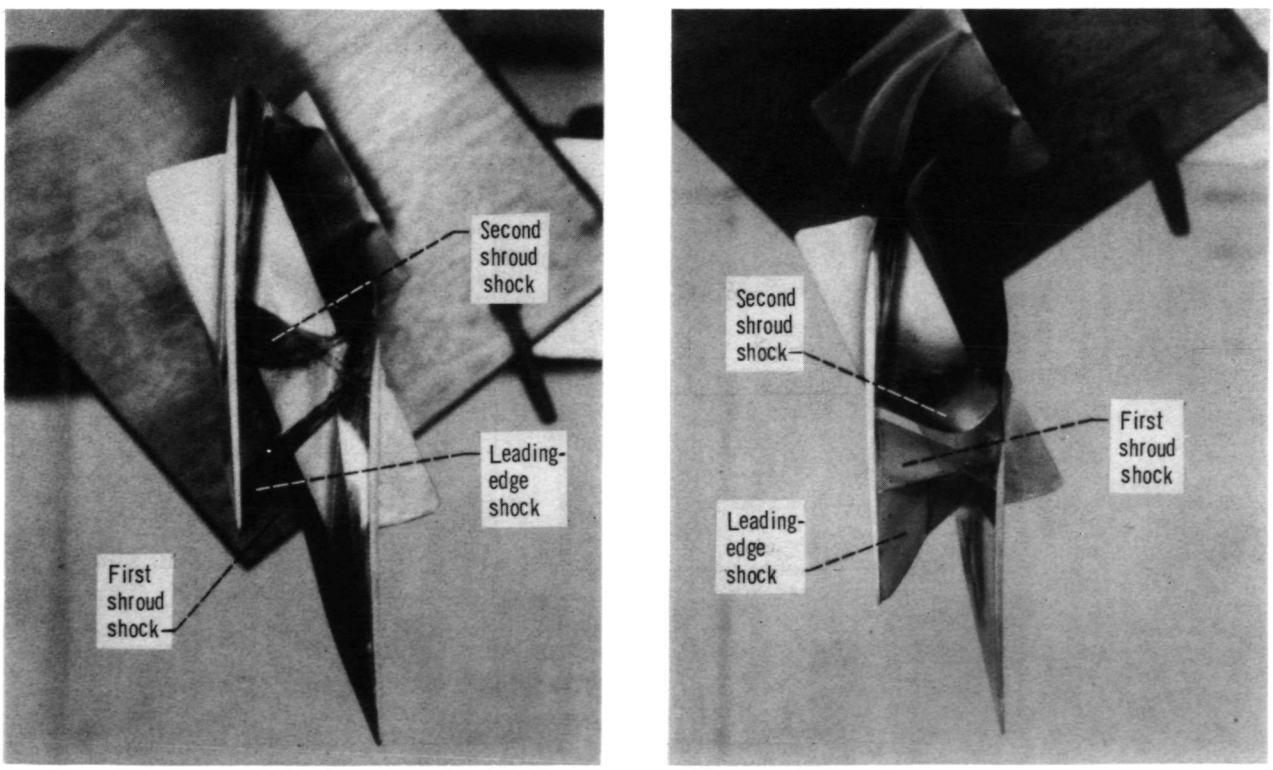

(a) Top view.

(b) Rear view.

Figure 5. - Views of 488.6-m/sec rotor blade model with shock system at design speed and near design pressure ratio.

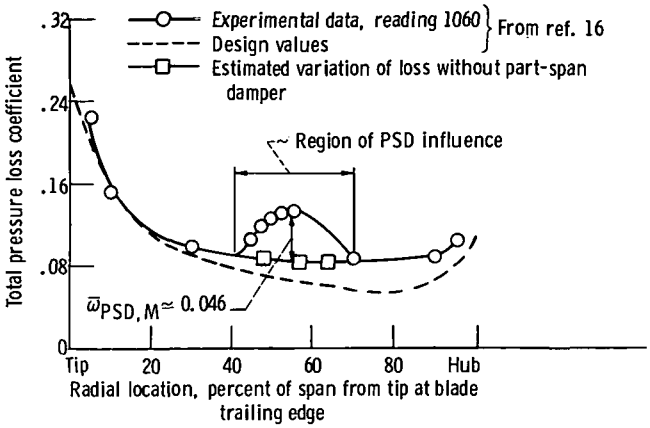

Figure 6. - Radial variation of total pressure loss coefficient for rotor 16 at design speed and maximum efficiency.

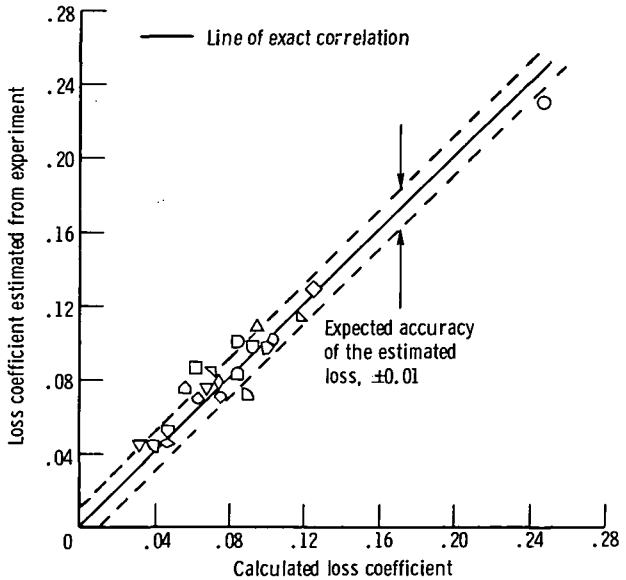

Figure 7. - Correlation of maximum total pressure loss coefficient due to part-span damper. (Symbols are identified in table I.)

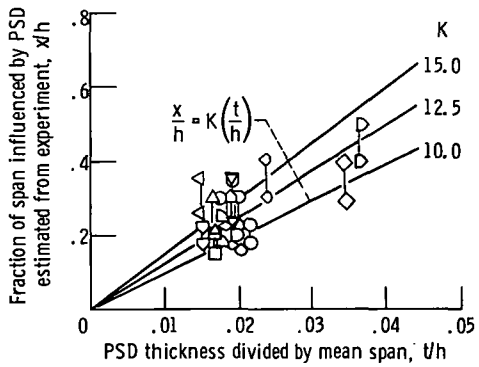

Figure 8. - Correlation of part-span damper relative thickness with fraction of span influenced. (Spread on x/h indicates tolerance on interpretation of data. Symbols are identified in table I.)

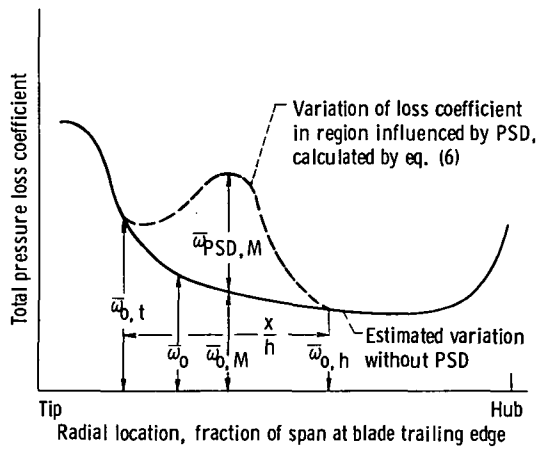

Figure 9. - Calculated spanwise variation of loss coefficient in region influenced by part-span damper. $\bar{\omega}_{PSD,M}$ from eqs. (3) and (4); x/h from eq. (5).)

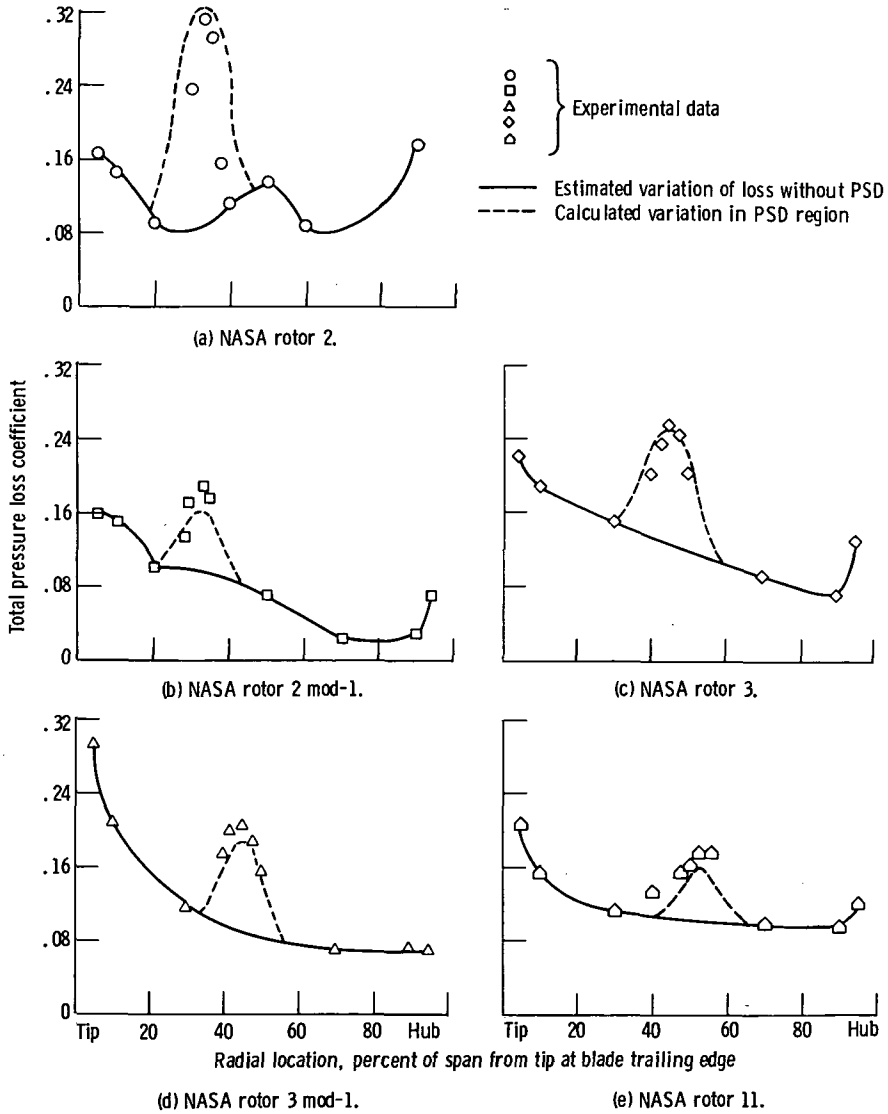

Figure 10. - Calculated radial variation of rotor loss coefficient in region influenced by part-span damper.

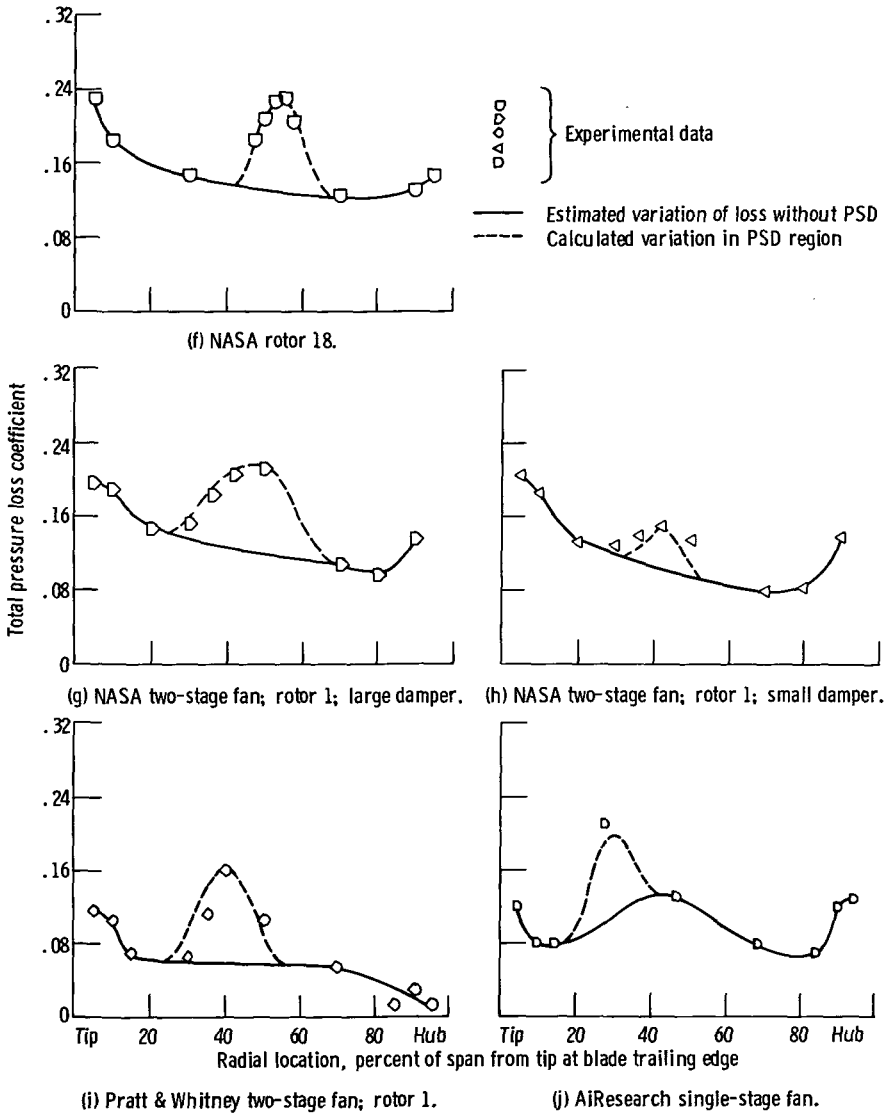

(f) NASA rotor 18.

(g) NASA two-stage fan; rotor 1; large damper.

(h) NASA two-stage fan; rotor 1; small damper.

(i) Pratt & Whitney two-stage fan; rotor 1.

(j) AiResearch single-stage fan.

Figure 10. - Concluded.

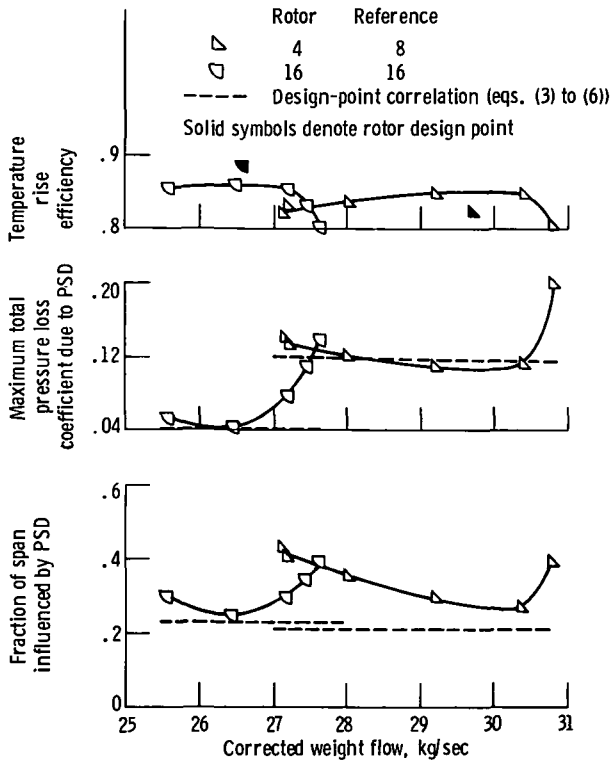

Figure 11. - Part-span damper (PSD) loss coefficient and region of influence as function of corrected weight flow for rotors 4 and 16.

NATIONAL AERONAUTICS AND SPACE ADMINISTRATION
WASHINGTON, D.C. 20546

OFFICIAL BUSINESS
PENALTY FOR PRIVATE USE $300

SPECIAL FOURTH-CLASS RATE
BOOK

POSTAGE AND FEES PAID
NATIONAL AERONAUTICS AND
SPACE ADMINISTRATION
451

U.S.MAIL

394 001 C1 U A 770527 S00903DS
DEPT OF THE AIR FORCE
AF WEAPONS LABORATORY
ATTN: TECHNICAL LIBRARY (SUL)
KIRTLAND AFB NM 87117

POSTMASTER: If Undeliverable (Section 158 Postal Manual) Do Not Return

"The aeronautical and space activities of the United States shall be conducted so as to contribute . . . to the expansion of human knowledge of phenomena in the atmosphere and space. The Administration shall provide for the widest practicable and appropriate dissemination of information concerning its activities and the results thereof."

—NATIONAL AERONAUTICS AND SPACE ACT OF 1958

NASA SCIENTIFIC AND TECHNICAL PUBLICATIONS

TECHNICAL REPORTS: Scientific and technical information considered important, complete, and a lasting contribution to existing knowledge.

TECHNICAL NOTES: Information less broad in scope but nevertheless of importance as a contribution to existing knowledge.

TECHNICAL MEMORANDUMS: Information receiving limited distribution because of preliminary data, security classification, or other reasons. Also includes conference proceedings with either limited or unlimited distribution.

CONTRACTOR REPORTS: Scientific and technical information generated under a NASA contract or grant and considered an important contribution to existing knowledge.

TECHNICAL TRANSLATIONS: Information published in a foreign language considered to merit NASA distribution in English.

SPECIAL PUBLICATIONS: Information derived from or of value to NASA activities. Publications include final reports of major projects, monographs, data compilations, handbooks, sourcebooks, and special bibliographies.

TECHNOLOGY UTILIZATION PUBLICATIONS: Information on technology used by NASA that may be of particular interest in commercial and other non-aerospace applications. Publications include Tech Briefs, Technology Utilization Reports and Technology Surveys.

Details on the availability of these publications may be obtained from:

SCIENTIFIC AND TECHNICAL INFORMATION OFFICE

NATIONAL AERONAUTICS AND SPACE ADMINISTRATION

Washington, D.C. 20546